Self-Similar Approach to Violent Relaxation

Richard N. Henriksen and Lawrence M. Widrow
Department of Physics Queen's University, Kingston, Canada, K7L 3N6

We consider the evolution of an initially cold, spherically symmetric system of self-gravitating particles. At early times the system undergoes self-similar collapse of the type described by Fillmore & Goldreich and Bertschinger. This stage of phase mixing soon gives way to a period of violent relaxation driven by an instability in the similarity solution. The onset of violent relaxation is illustrated by numerical simulations and supported by non-linear analysis of the "scaled" collisionless Boltzmann and Poisson equations.

The early evolution of an initially cold, self-gravitating system of collisionless particles is governed by two dynamical processes: phase mixing and violent relaxation [1]. With phase mixing, the initial, single-velocity stream distribution function is wound into a tight spiral pattern that can be described ultimately as a smooth (i.e., coarse-grained) function of the phase space variables $\mathbf{x}$ and $\mathbf{v}$. With violent relaxation [2], the energies of individual particles in the distribution function (DF) change as they move through the time-dependent potential of the collapsing object. Violent relaxation leads to a more rapid and complete mixing of the DF and may erase all memory of initial conditions [2,3].

Clearly both phase mixing and violent relaxation operate during the formation of gravitationally bound systems. However the precise role each plays in the relaxation process is largely unknown [4]. Moreover it is not known whether realistic systems such as dark matter galactic halos are truly mixed. The question is important for dark matter search experiments where the DF for the dark matter particles is almost always treated as a smooth function of $\mathbf{x}$ and $\mathbf{v}$ (see however reference [5]).

Fillmore & Goldreich [6] and Bertschinger [7] have found similarity solutions which describe the collapse of initially cold, spherically symmetric perturbations in an expanding universe. While their solutions exhibit some features of violent relaxation (particle energies change as they move through a time-dependent potential) the essential physics is that of phase-mixing. In particular the self-similar DFs found are characterized by a single thread in phase space.

In this paper we demonstrate that the similarity solutions of [6,7] are unstable and that the instability leads to true violent relaxation of the system. We begin by formulating the problem of self-similar collapse in a novel way working directly with the DF rather than particle orbits. For simplicity we impose spherical symmetry and treat only radial orbits. The DF then depends on three variables; radius, radial velocity, and time. A scaling symmetry is imposed which reduces, by one, the number of independent variables in the collisionless Boltzmann equation (CBE). The resultant equations are characterized by a single dimensionless parameter which can be related to the profile of the initial mass distribution. Not surprisingly, the characteristics of the CBE correspond to the orbit equations derived in [6,7]. However the interpretation is different and leads to a deeper understanding of the problem. We next perform N-body simulations of spherical radial collapse following the orbits of particles (i.e., spherical shells) directly in phase space. Early on the DF exhibits characteristics of the self-similar solutions found in [6,7]. However an instability soon develops leading to efficient mixing of the DF.

The collisionless Boltzmann and Poisson equations for a spherically symmetric system are

$$\partial_t f + v_r \partial_r f + \left(\frac{j^2}{r^3} - \partial_r \Phi\right)(\partial_{v_r} f) = 0 \ , \tag{1}$$

$$\partial_r (r^2 \partial_r \Phi) \ = \ 4\pi^2 \int dj^2 \int f(r, v_r, j^2)\, dv_r \tag{2}$$

where f is the phase space mass density and Φ the is 'mean field' gravitational potential. For purely radial orbits we introduce the canonical distribution function $F(t, r, v_r)$ where $f \equiv \left(4\pi r^2\right)^{-1} \delta(j^2) F$. The equations then become:

$$\partial_t F + v_r \partial_r F - \partial_r \Phi \ \partial_{v_r} F = 0 \tag{3}$$

$$\partial_r \left(r^2 \partial_r \Phi \right) \ = \ G \int F \, dv_r \ . \tag{4}$$

We assume that a scaling symmetry exists along a direction $\mathbf{k}$ where [8,9]

$$k^j \partial_j \ = \ t\partial_t \ + \ \delta r \partial_r \ + \ \nu v_r \partial_{v_r} \tag{5}$$

and δ and ν are real parameters. It is convenient to introduce an oblique time parameter $T(t)$ such that $k^j \partial_j T = 1$. Self-similarity is imposed by requiring that all dimensional quantities scale along $\mathbf{k}$ according to $A = A_o \exp \beta T$ where β depends on δ and ν and on the dimensionality of A. Applying this procedure to the independent variables r and v_r and to the dependent variables F and Φ we find

$$\nu \overline{F} + (Y - \delta X) \frac{\partial \overline{F}}{\partial X} - \left(\nu Y + \frac{d\overline{\Phi}}{dX} \right) \frac{\partial \overline{F}}{\partial Y} = 0 \tag{6}$$

$$\frac{d}{dX} \left(X^2 \frac{d\overline{\Phi}}{dX} \right) \ = \ \int \overline{F} dY \tag{7}$$

where $r = e^{\delta T} X$, $v_r = e^{\nu T} Y$, $F = G^{-1} e^{\nu T} \overline{F}$, $\Phi = e^{2\nu T} \overline{\Phi}$, and $\nu = \delta - 1$. δ is set by initial conditions as illustrated in the following simple example. Consider a system which evolves from a cloud of particles whose initial density distribution is $\rho = \lambda r^{-\epsilon}$ where λ and ϵ are constants. We expect the self-similar development to 'remember' a kinematical constant $G\lambda$ whose dimensions are given by $[G\lambda] = (\mathit{length})^{\epsilon} / (\mathit{time})^2$. Our general solution 'remembers' a kinematical constant $X \propto r/t^{\delta}$ as this is invariant under the symmetry Eq. (5). This leads to the correspondence $\epsilon = 2/\delta$.

Eqs. (6,7) are difficult to solve by direct methods in part because of the complicated boundary conditions (e.g., the DF should be continuous at $X \to 0$ as one passes from large negative Y (ingoing particles) to large positive Y (outgoing particles)). Instead we consider the characteristic curves of the system:

$$\frac{dX}{ds} = Y - \delta X \ ; \quad \frac{dY}{ds} = (1-\delta) Y - \frac{d\overline{\Phi}}{dX} \ , \tag{8}$$

$$\frac{d\overline{F}}{ds} \ = \ (1-\delta) \overline{F} \tag{9}$$

where s is the path increment along a given curve. Eq. (9) leads immediately to the result $\overline{F} \ = \ e^{(1-\delta)s} \mathcal{F}(\zeta)$ where $\zeta(X,Y)$ is constant along a characteristic. The differential equations for X and Y can be combined to obtain a single second order differential equation

$$\frac{d^2X}{ds^2} \ + \ (2\delta - 1) \frac{dX}{ds} \ + \ \frac{d\overline{\Phi}_{\text{eff}}}{X} \ = \ 0 \tag{10}$$

where $\overline{\Phi}_{\text{eff}} \equiv \overline{\Phi} + \delta(\delta - 1) X^2/2$. While this equation is formally equivalent to the orbit equations derived in [6,7] the interpretation is different. In particular the DF in [6,7] consist of particles that lie along a single characteristic (i.e., $\delta-$function of ζ) as opposed to the smooth function $\overline{F} = \overline{F}(X,Y)$ given by the solution to Eqs. (6,7).

The DFs found in [6,7] describe an eternal self-similar collapse but say little about how the system enters or exits such a phase. Moutarde et al. [10] have found features of the similarity solutions in cosmological N-body simulations of initial overdensities concluding that self-similar behavior of this type is ubiquitous in local collapses. Along different lines simple physical arguments [11] as well as numerical simulations [12] can be used to suggest analytic models for the final DF of violently-relaxed galaxies.

Our numerical experiments set out to observe, directly in phase space, the onset of self-similar behavior as well as the transition to a final equilibrium configuration. We model a spherically symmetric distribution of particles traveling on purely radial orbits using a shell code. The initial density profile is characterized by a power-law function of r; $\rho_i \propto r^{-\epsilon}$ $(0 < \epsilon < 3)$. Potential difficulties at $r \to 0$ are treated by using a softened force law $\propto M(r)/(r^2 + r_0^2)$ where $M(r)$ is the mass interior to r. Alternatively we can place a reflecting sphere at the origin or include a small amount of angular momentum. Fig. 1 gives the phase space coordinates of all shells in the simulation at six different times starting from an initial density profile characterized by $\epsilon = 3/2$. For this experiment we set $G = M(\infty) = 1$ and use a softened force law with $r_0 = 0.01$. Panels b and c illustrate the essential behavior of the self-similar solutions. The distribution function in panel c is almost identical to that of panel b provided we scale r by a factor $s = 1.8$ and v_r by a factor $s^{\nu/\delta} = s^{1/4}$ where that latter scaling is set by the relations $\delta = 2/\epsilon$ and $\nu = \delta - 1$. Similar results are found for an initial density profile $\rho \propto r^{-5/2}$ where the velocity scale factor is $s^{-1/4}$ for a position space scale factor s. These results confirm the presence of self-similarity as well as the connection established above between the initial density profile and δ.

Panels d and e illustrate new and unexpected behavior. Evidently there is an instability in the similarity solution. Fluctuations driven by this instability grow in time and quickly lead to mixing of particles between neighboring streams erasing much of the fine-grained spiral pattern. Interestingly enough the pattern of instability is replicated along the outer streams in the DF as one might expect given the self-similar nature of the evolution. We have checked that this instability is real by varying the timestep by a factor of 100 and the number of shells by a factor of 16 ($N = 1000$ to $N = 16,000$) and find that the quantitative features of the instability remain the same. In addition very similar results arise in the $\rho_i \propto r^{-5/2}$ runs where a different shell spacing is used. The onset of the instability is sensitive to r_0 and can be delayed by making r_0 bigger. Likewise adding a small amount of angular momentum will delay growth of the fluctuations. This is the expected result since violent relaxation requires particles to move through a rapidly varying potential which, for our example, is present at the origin. Indeed the equilibrium DFs constructed in [3,11] were based on this premise.

Our initial DF is finite in extent which leads to some interesting effects. In panel e the last particles have fallen through the center and are now on their way toward apapsis. However there are no more particles falling in for the first time and so these last few particles are less tightly bound than their earlier counterparts. The end of the distribution is therefore flung out to large radii like the end of a whip. Panel f shows the late time behavior of the system. The phase space density at small r is now quite smooth with no evidence of the earlier fine-grained structure found in [6,7]. The outer regions of the DF are characterized by a strikingly narrow stream of particles. These are the last few particles discussed above. Most are loosely bound and will eventually fall back into the main distribution signaling a second round of secondary infall.

We find, in agreement with [10], that all cases where the initial density law is shallower than $\epsilon = 2$ have a density profile during the self-similar phase $\propto r^{-2}$. Alternatively, when the initial density law is steeper than $\epsilon = 2$, the self-similar slope is equal to the initial slope. The existence of two distinct cases was noted originally in [6] and also in [10] and is discussed below in the context of the non-linear dynamical analysis.

Eqs. (8) yield the characteristics of a presumed smooth, scaled, DF with F along a characteristic given by the solution to Eq. (9). However the equivalent second order equation (14) reveals that this system is not integrable unless the 'friction' term $(2\delta - 1)dX/ds$ is either negligible or exactly zero. The exactly integrable case ($\delta = 1/2$) corresponds to the condition that the assumed self-similar symmetry (6) be an infinitesimal canonical transformation generated by the radial action. Our dimensional argument suggests that this case corresponds to the unphysical initial density profile with $\epsilon = 4$. In fact we show in a subsequent paper that it is best associated with a distribution of particles having constant angular momentum throughout. For general δ the friction term becomes negligible at small X.

When the non-integrability is manifest (the spiral 'phase mixing' orbits in phase space such as that shown in Figs. (1b,c)) the functions $\zeta(X, Y)$ and $s_\zeta(X, Y)$ are not canonical coordinates and can not be used to define a phase space volume element everywhere. Consequently the DF is not defined over the whole phase space. In the integrable limit ($X \to 0$) it becomes possible to partition phase space with ζ (which becomes an 'energy' integral) and s_ζ. The evolution towards the existence of a smooth DF parallels the numerical relaxation that we have observed in Fig. 1.

The other essential element for the existence of a smooth DF is coarse graining. The fine-grained volume element must remain strictly zero in the simulation, since the particles begin from rest. Nevertheless a combination of round-off error and real instability leads to a diffusion of this volume element throughout integrable phase space (e.g. Fig. 1f). This corresponds to the increase in entropy associated with coarse grained DF's. The coarse graining formally consists in taking the integrable characteristics to be dense in phase space.

Fig. 2 shows the topological structure of the characteristic curves assuming the friction term is negligible. For $\delta < 1$ (the case shown in the figure) there is a singular point at $Y = \delta X$ and $d\overline{\Phi}_{eff}/dX = 0$ i.e., simultaneously a turning point and an extremum in the effective potential. It is easy to show that this is a saddle point. At infinity there are two more singular points, one stable node and one unstable node. These connect in a straightforward way to the curves of Fig. 2. In this case ($\epsilon > 2$) the numerical experiments indicate that the initial density distribution is imported into the self-similar region. When $\delta > 1$ the effective potential increases monotonically and there are no singular points at finite X. Moreover one finds that the stable node at infinity is replaced by a saddle while the unstable node remains unchanged. It is as though the region of violent-relaxation extends to infinity. The numerical experiments show that in this case all memory of the initial density distribution is lost in favor of a universal profile that is close to r^{-2}. (Our analysis suggests that a universal profile $\rho(r) \propto r^{-2}t^{-1}\left(\log r/t^{1/2}\right)^{-1/3}$ during the collapse phase. The logarithmic correction factor is reminiscent of what is found in the equilibrium models [11]. At present our numerical simulations do not have the dynamic range to verify this.) Fillmore & Goldreich describe $\delta < 1$ as the case where the inner halo is dominated by particles with small apapsis and $\delta > 1$ as the case where particles are spread throughout the halo in agreement with the discussion above.

The connection between the topology of the coarse-grained DF and the ultimate density law in the self-similar region leads us to suggest that *the appropriate pair of separatrices of the saddle point form an effective boundary to the violently relaxed region of phase space (and hence to the region of entropy increase).* By contrast the radial instability, which seems to be the principal mechanism for relaxation in phase space, is present quite independently of the topology of the DF characteristics.

Our results provide a simple yet dramatic example of the interplay between phase mixing and violent relaxation. The next step will be to include angular momentum, deviations from spherical symmetry, and small-scale clumpiness with the hope of better understanding the formation and structure of realistic systems.

We are grateful to J. Dursi for help with the numerical simulations and to M. Duncan, M. H. Lee, S. Tremaine, and G. Holder for valuable conversations. This work was supported in part by the Natural Science and Engineering Research Council of Canada.

---

[1] J. Binney and S. Tremaine, *Galactic Dynamics* (Princeton University Press, Princeton, New Jersey, 1987).
[2] D. Lynden-Bell, Mon. Not. R. Astron. Soc. **136**, 101 (1967).
[3] S. Tremaine, in *Structure and Dynamcis of Elliptical Galaxies* edited by T. de Zeeuw (Reidel Pub. Co., Dordrecht, Netherlands, 1986).
[4] D. Merritt and M. Valluri, Astrophys. J. **471**, 82 (1996).
[5] P. Sikivie, I. I. Tkachev, and Y. Wang, FERMILAB-Pub-96/286-A (1996).
[6] J. A. Fillmore and P. Goldreich, Astrophys. J. **281**, 1 (1984).
[7] E. Bertschinger, Astrophys. J. Suppl. **58**, 39 (1985).
[8] B. Carter and R. N. Henriksen, J. Math. Phys. **32**, 2580 (1990).
[9] R. N. Henriksen and L. M. Widrow, Mon. Not. R. Astron. Soc. **276**, 679 (1996).
[10] F. Moutarde, J.-M. Alimi, F. R. Bouchet, and R. Pellat, Astrophys. J. **441**, 10 (1995).
[11] D. Merritt, S. Tremaine, and D. Johnstone, Mon. Not. R. Astron. Soc. **236**, 829, (1989).
[12] L. A. Aguilar and D. Merritt, Astrophys. J. **354**, 33 (1990).

FIGURE 1: Evolution of a system of particles in phase space (r, v_r) starting with zero velocity. $G = M(\infty) = 1$ which sets the units for radius, time, and velocity. The initial density profile is $\propto r^{-3/2}$. Panels a-f correspond to $t = 0.0, 0.4, 0.6, 1.0, 1.2, 5.6$.

FIGURE 2: Phase diagram for the characteristic curves of the self-similar CB and Poisson equations with $\delta = 0.8$ ($\epsilon = 5/2$). The star marks the saddle point discussed in the text. Inset: Effective potential $\Phi_{\rm eff}$ as a function of $\log_{10}(X)$. Solid and dotted curves are for $\epsilon = 5/2$ and $3/2$ respectively.

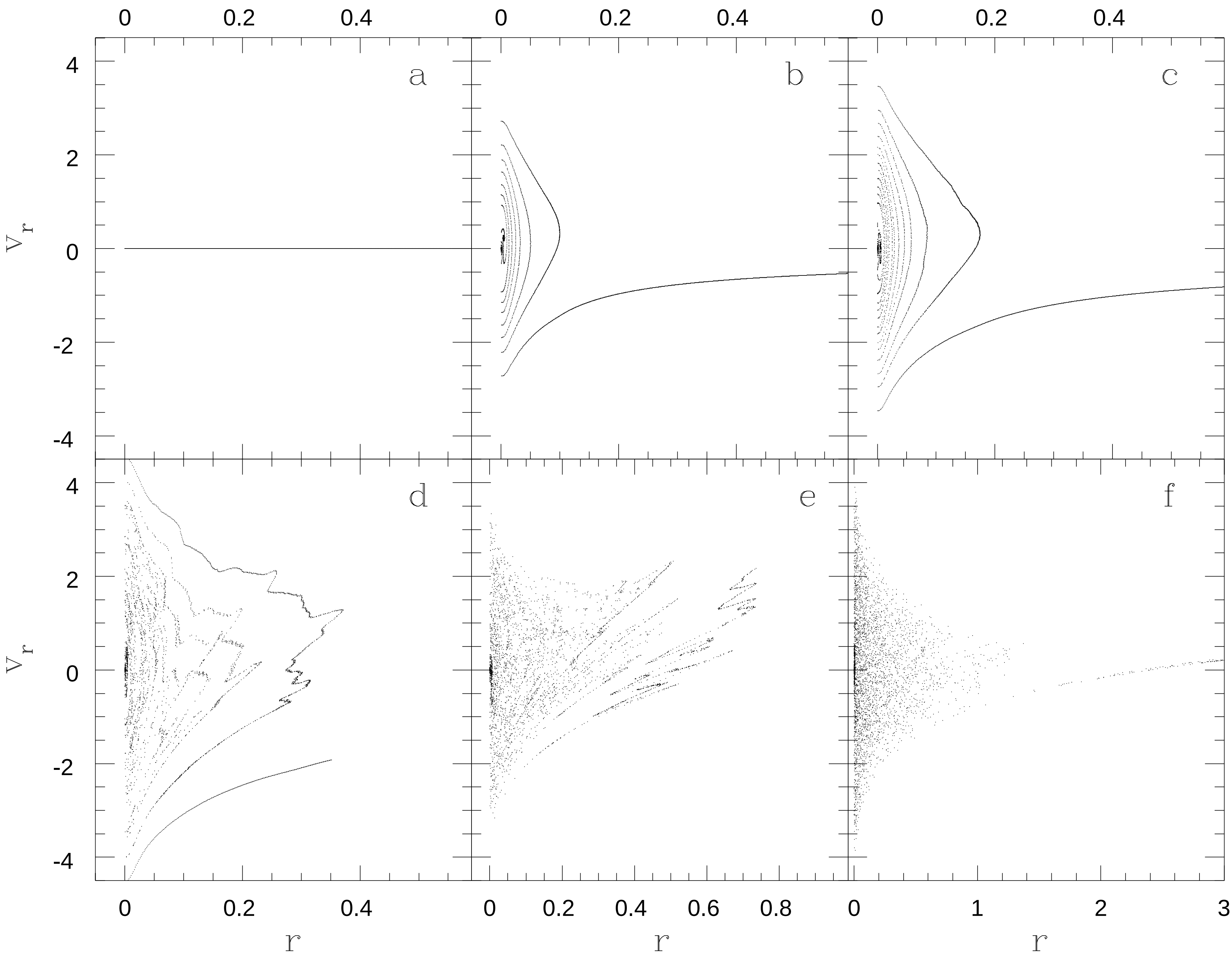
a
b
c
d
e
f
V_r
V_r
r
r
r
0
0.2
0.4
0.6
0.8
1
2
3
4
2
-2
-4

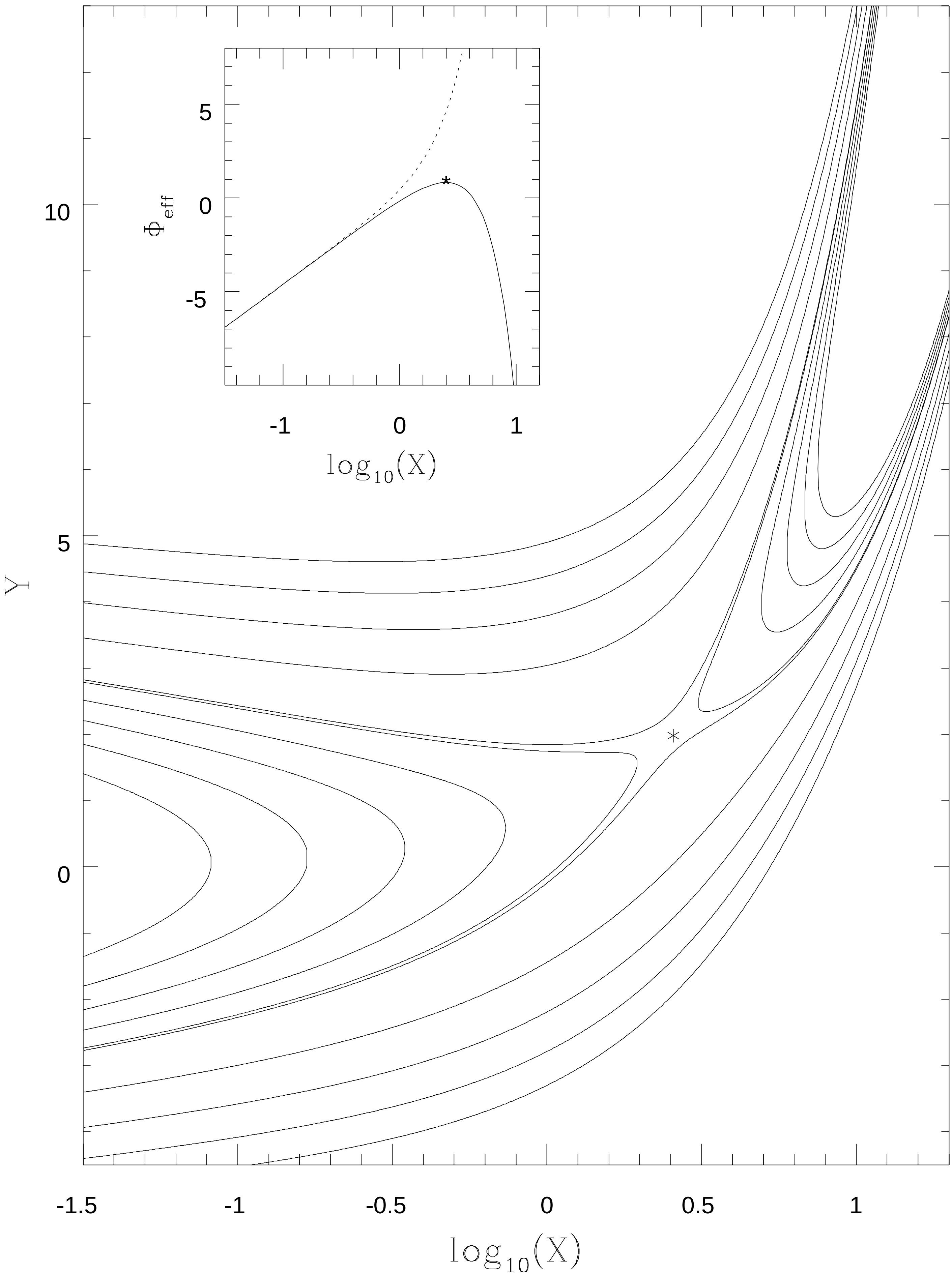

Φ_eff
5
0
-5
-1
0
1
log10(X)
10
5
0
Y
-1.5
-1
-0.5
0
0.5
1
log10(X)